Localized Delivery of a Photosensitizer using Dissolvable Microneedle Patch for Oral Cancer Treatment

Rupal Kothari [a], Neha K Nambiar [b], Vibhawari Pundir [b], Manab Chakravarty [b], Danaboniya Ramaiah [b], Amit Nag [b], and Vamsi Krishna Venuganti*[a]

[a] Department of Pharmacy, BITS-Pilani Hyderabad Campus, Hyderabad, India -500078
[b] Department of Chemistry, BITS-Pilani Hyderabad Campus, Hyderabad, India -500078
*[a] Corresponding author e-mail: **vamsi@hyderabad.bits-pilani.ac.in**

Introduction

Oral cancer, accounting for 85% of head and neck cancers, presents a growing global health burden with increasing incidence and mortality. Cancer treatments like chemotherapy, radiation, and immunotherapy face limitations such as side effects and poor efficacy. Phototherapy offers a safer alternative with lower toxicity and greater selectivity attributed to the activation of photosensitizers (PSs) by light to produce photothermal (PTT) or photodynamic effects (PDT). However, challenges such as suboptimal PS accumulation and dark cytotoxicity limit its clinical application.

Objective

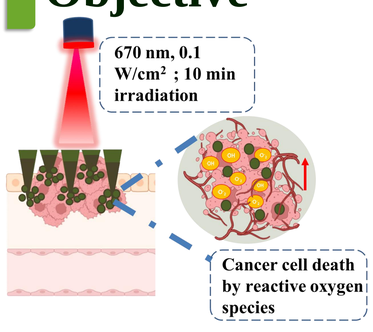

This study explores the integration of aza-BODIPY (AZP10) into dual-length dissolvable MNs (AZP10 DMN) for site-specific delivery in buccal tissues, demonstrating the potential for localized oral cancer treatment via 670 nm laser irradiation.

Methodology

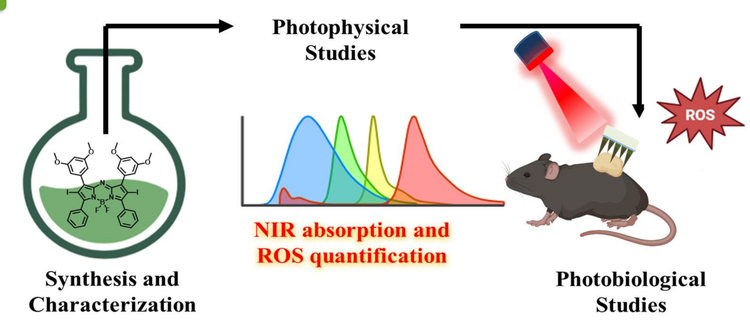

Results and discussion

Design and synthesis

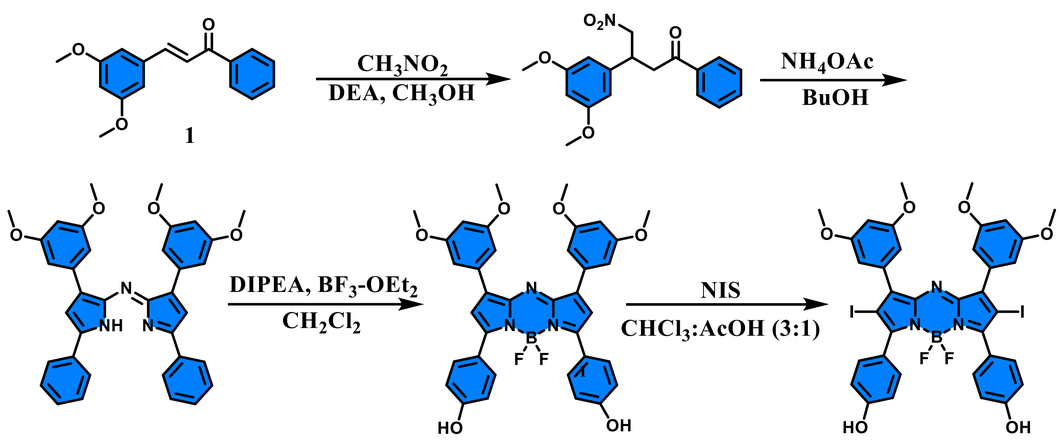

Figure 1: Schematic outline for the synthesis of core iodinated aza BODIPY (AZP10)

Photophysical characterization

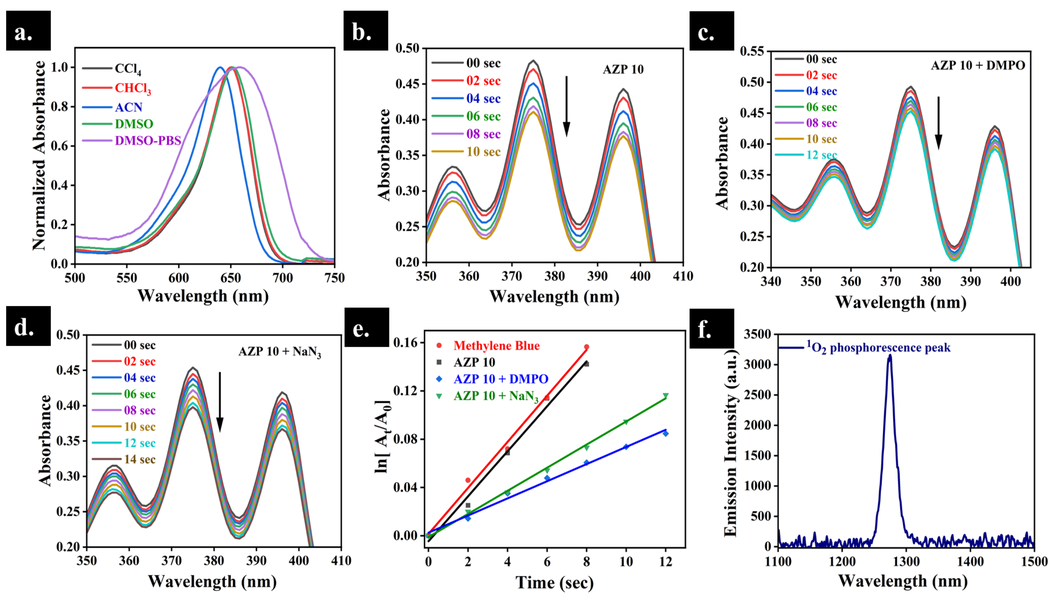

Figure 2. a) Absorption spectra of AZP10 in different solvents. Degradation of DMA under 670 nm irradiation (100 mW/cm^2) in the presence of AZP10 in b) DMSO-PBS, c) in the presence of AZP10-DMPO in DMSO-PBS, and d) presence of AZP10-NaN_3 in DMSO-PBS. e) The plot of ln(At/A0) vs. time to calculate the slopes for degradation of DMA. (f) Phosphorescence spectrum of in situ generated $^1O_2$, when AZP10 in $CDCl_3$ was excited at 651 nm

Photobiological studies

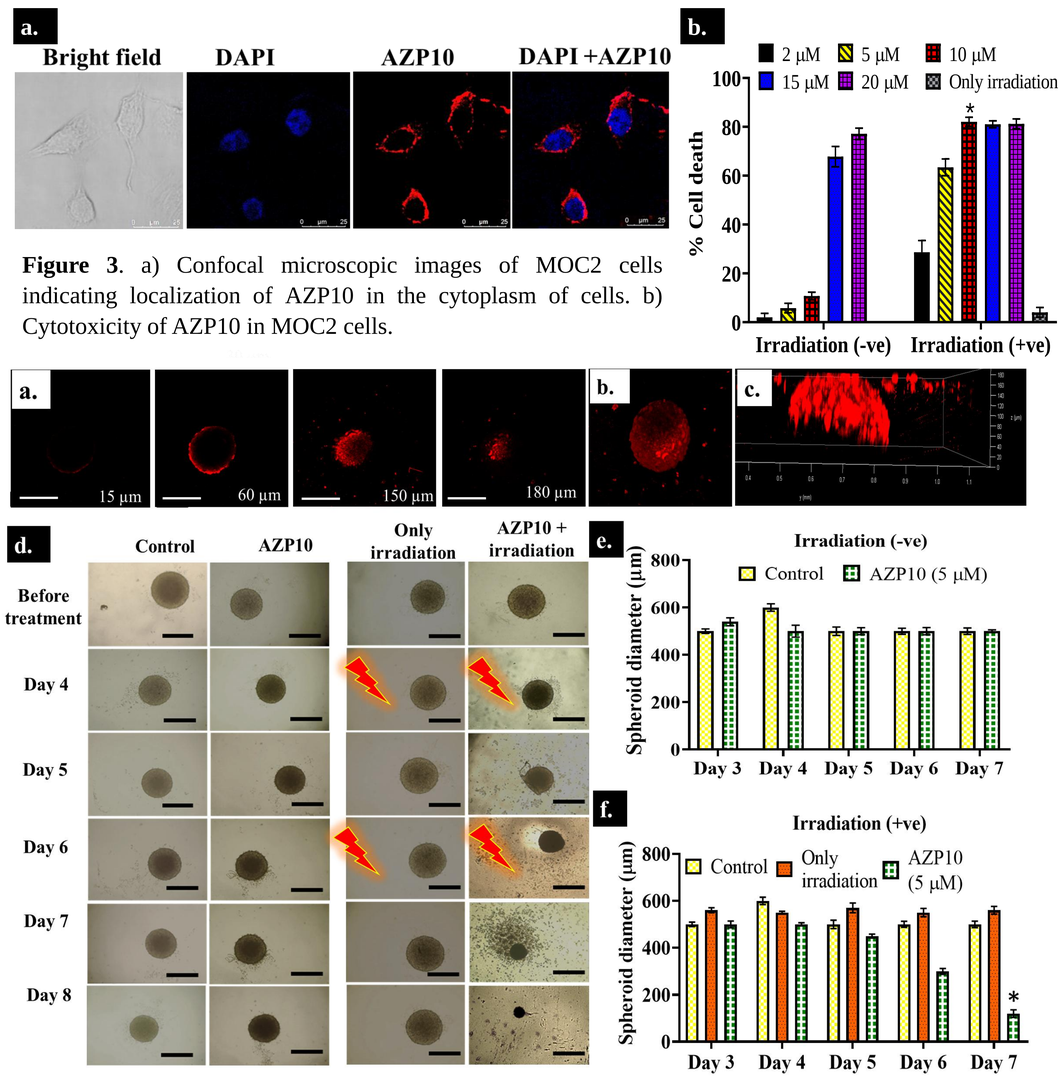

Figure 3. a) Confocal microscopic images of MOC2 cells indicating localization of AZP10 in the cytoplasm of cells. b) Cytotoxicity of AZP10 in MOC2 cells.

Figure 4. a) Two-photon laser scanning XYZ optical sections from the surface of the FaDu spheroid incubated with AZP10 (5 µM) for 4 h. b) 3D stacked image of spheroid. c) Surface to depth penetration of AZP10 by Z stack. d) Optical microscopic images of FaDu spheroids with and without irradiation (670 nm, 100 mW/cm^2; 10 min) in the presence of AZP10 (5 µM) incubated for 4 h. e) and f) Reduction in spheroid diameter for dark control and AZP10-irradiated group respectively

Figure 5. a) CAD design of master mold. Digital photograph of b) 3D printed resin master mold, c) PDMS mold, d) blank PVA-PVP DMN patch. e) Confocal laser scanning microscopic images of optical sections of the excised porcine buccal mucosa after application of AZP10 DMN. f and g) Confocal laser scanning microscopic images of DMN before and after insertion into the excised porcine buccal mucosa. h) 3D stacking of AZP10 DMN. i) 3D stack showing insertion of DMN into the mucosa.

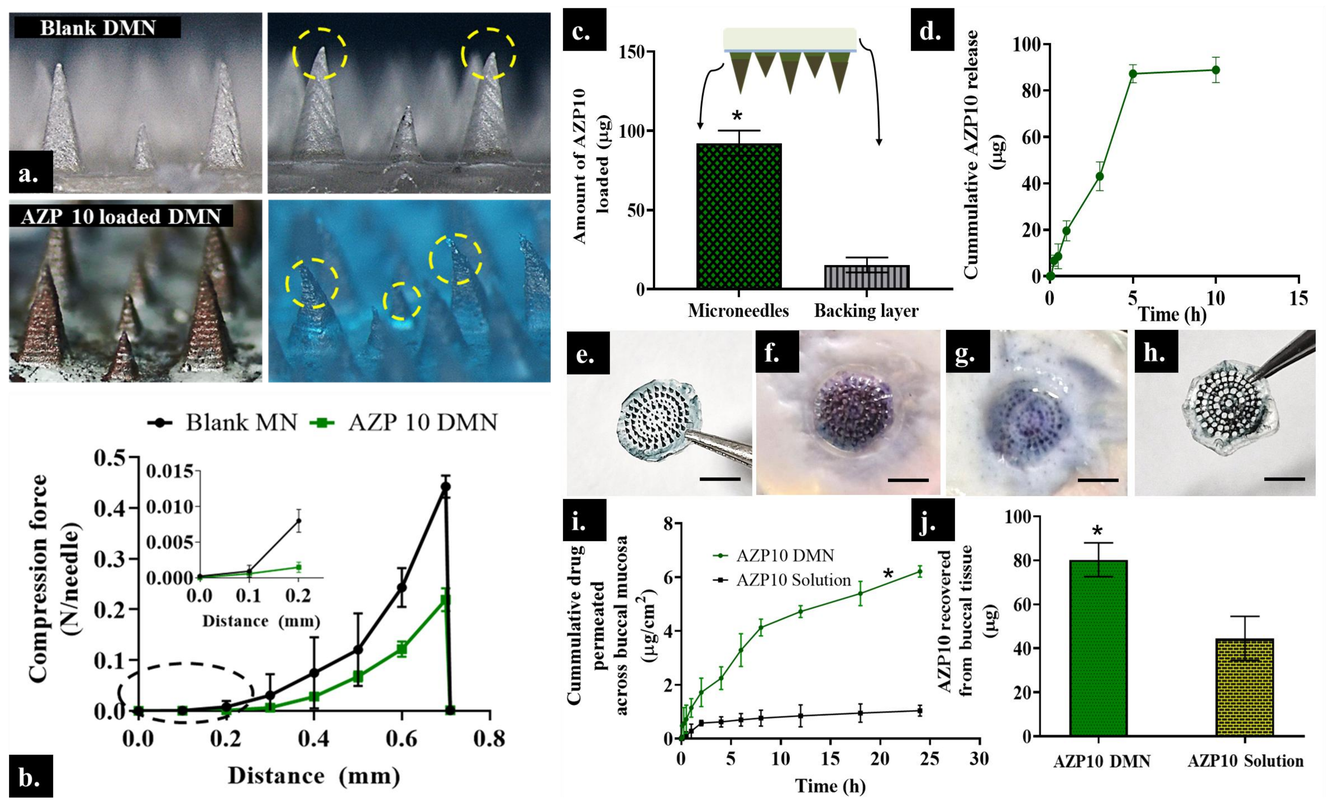

Figure 6. a) Force-displacement graphs obtained from the compression test of DMN using the texture analyzer. b) Stereomicroscopic images of blank and AZP10 DMN after compression test. c) The amount of AZP10 present in microneedles and the backing layer. d) Release profile of AZP10 from AZP10 DMN upon dissolution in PBS containing 0.5% Tween 80. e) Digital photograph of AZP10 DMN. f) Application of AZP10 DMN on the excised porcine buccal mucosa. g) The porcine buccal mucosa after AZP10 DMN removal. h) Recovered backing layer indicating dissolved needles. i) Cumulative amount of AZP10 permeated across the excised porcine buccal mucosa after application of AZP10 DMN and AZP10 solution. j) The amount of AZP10 retained within the buccal mucosa after application of DMN and solution.

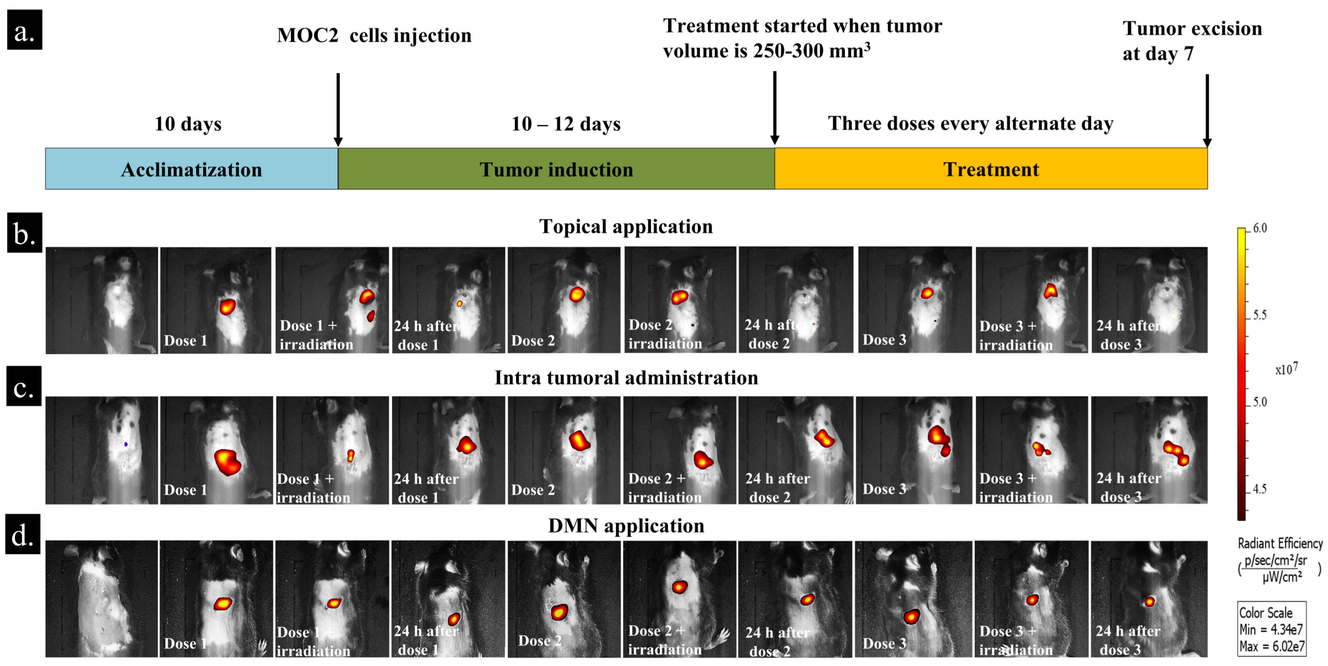

Figure 7. a) Schematic of the timeline of the tumor inhibition study in C57BL/6 mice. Representative i*n vivo* NIR fluorescence images of tumor-bearing mice of b) topical application group, c) intratumoral group, and d) AZP10 DMN application group

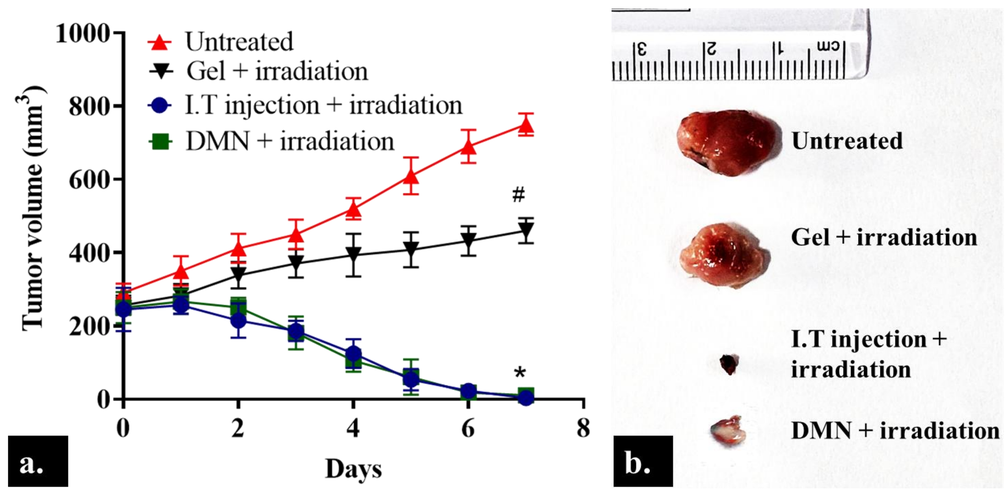

Figure 8. a) The change in tumor volume with time after irradiation of AZP10 administered with topical gel, intratumoral injection, and DMN. b) Representative digital photographs of excised tumors on day 7

Conclusion

This study introduces a photosensitizer with superior photophysical properties and dual-length dissolving microneedles (DMNs) for minimally invasive oral cancer treatment. The DMNs optimize drug delivery to both superficial and deeper tumor regions. AZP10 DMNs achieved significant tumor regression in mice after three irradiation cycles, comparable to intratumoral injection and superior to topical gel application.

Acknowledgement

Department of BioTechnology, Government of India
सत्यमेव जयते
विज्ञान एवं प्रौद्योगिकी मंत्रालय
MINISTRY OF SCIENCE AND TECHNOLOGY
सत्यमेव जयते